2016

Antibody response to the hypervariable region-1 interferes with broadly neutralizing antibodies to hepatitis C virus

Zhen-yong Keck
Stanford University School of Medicine

Christine Girard-Blanc
Institut Pasteur

Wenyan Wang
Stanford University School of Medicine

Patrick Lau
Stanford University School of Medicine

Adam Zuiani
Institut Pasteur

See next page for additional authors

JVI Accepted Manuscript Posted Online 6 January 2016
J. Virol. doi:10.1128/JVI.02458-15

Antibody response to the hypervariable region-1 interferes with broadly neutralizing antibodies to hepatitis C virus

Zhen-yong Keck[1], Christine Girard-Blanc[2,3], Wenyan Wang[1], Patrick Lau[1], Adam Zuiani[6], Felix A Rey[4,5], Thomas Krey[4,5,&], Michael S. Diamond[6,7,8] and Steven K.H. Foung[1#]

[1]Department of Pathology, Stanford University School of Medicine, Stanford, CA 94305

[2]Institut Pasteur, Proteopole and [3]CNRS UMR 3528, Paris, France

[4]Institut Pasteur, Unité de Virologie Structurale, Department Virologie and [5]CNRS UMR 3569, Paris, France

Departments of Pathology and Immunology[6], Medicine[7] and Molecular Microbiology[8], Washington University School of Medicine, St. Louis, MO 63110

[&]Present address: Institute of Virology, Hannover Medical School, Hannover, Germany

Short Title: Anti-HVR1 antibodies interfere with broadly neutralizing antibodies

Keywords: Hepatitis C virus, neutralizing human monoclonal antibodies, anti-HVR1, E2 glycoprotein, viral escape

[#]Corresponding Author

Stanford Blood Center

3373 Hillview Avenue

Palo Alto, CA 94304

Phone: (650) 723-6481

Fax: (650) 725-6610

E-mail: sfoung@stanford.edu

ABSTRACT

The hypervariable region-1 (HVR1) (amino acids (aa) 384-410) on the E2 glycoprotein of hepatitis C virus contributes to persistent infection by evolving escape mutations that attenuate binding of inhibitory antibodies and by blocking access of broadly neutralizing antibodies to their epitopes. A third proposed mechanism of immune antagonism is that poorly neutralizing antibodies binding to HVR1 interfere with binding of other superior neutralizing antibodies. Epitope mapping of human monoclonal antibodies (HMAbs) that bind to an adjacent, conserved domain on E2 encompassing aa 412-423 revealed two subsets, designated as HC33 HMAbs. While both subsets have contact residues within aa 412-423, alanine scanning mutagenesis suggested that one subset, which includes HC33.8, has an additional contact residue within HVR1. To test for interference of anti-HVR1 antibodies with binding of antibodies to aa 412-423 and other E2 determinants recognized by broadly neutralizing HMAbs, two murine MAbs against HVR1 (H77.16) and aa 412-423 (H77.39) were studied. As expected, H77.39 inhibited the binding of all HC33 HMAbs. Unexpectedly, H77.16 also inhibited the binding of both subsets of HC33 HMAbs. This inhibition also was observed against other broadly neutralizing HMAbs to epitopes outside of aa 412-423. Combination antibody neutralization studies by the median-effect analysis method with H77.16 and broadly reactive HMAbs revealed antagonism between these antibodies. Structural studies demonstrated conformational flexibility in this antigenic region, which supports the possibility of anti-HVR1 antibodies hindering the binding of broadly neutralizing MAbs. These findings support the hypothesis that anti-HVR1 antibodies can interfere with a protective humoral response against HCV infection.

Importance. The HVR1 contributes to persistent infection by evolving mutations that escape from neutralizing antibodies to HVR1 and by shielding broadly neutralizing antibodies from their epitopes. This study provides insight into a new immune antagonism mechanism by which the binding of antibodies to HVR1 blocks the binding and activity of broadly neutralizing antibodies to HCV. Immunization strategies that avoid the induction of HVR1 antibodies should increase the inhibitory activity of broadly neutralizing anti-HCV antibodies elicited by candidate vaccines.

INTRODUCTION

Up to 170 million people worldwide are infected with hepatitis C virus (HCV) with significant risk for liver failure and hepatocellular carcinoma. The World Health Organization estimates an annual increase in the global burden by two million new infections (40) and in the United States HCV is increasing in young adults from injection drug use (25). Multiple lines of evidence suggest that CD4+ and CD8+ T cell responses are needed to control acute infection but insufficient to prevent long-term persistence (2). Accumulating data indicate that neutralizing antibodies are an important correlate of HCV clearance. In chimpanzee studies, an infectious inoculum obtained during acute infection from a patient who eventually developed chronic HCV hepatitis could be neutralized by *in vitro* incubation with plasma of the same subject collected at 2 years after the initial infection (12). A neutralizing antibody response measured against pseudotyped retroviral particles expressing HCV E1E2 glycoproteins (HCVpp) has been associated with control of infection in single source outbreaks of acute HCV infections (35). In addition, antibodies to HCV E2 prevent (28, 32) and clear established infection (8) in a human liver-mouse chimeric model. In spite of the relationship between antibodies and protection against HCV infection, 10^4-10^6 virions per milliliter of serum can be detected during chronic infection even in the presence of high levels of neutralizing antibodies in serum.

One driver of persistent viremia is a high degree of viral variants or "quasispecies". From a viral replication rate of 10^{12} copies per day with an error prone NS5B RNA-dependent polymerase, the estimated mutation rate is $2.0X10^{-3}$ base substitutions per genome per year (4). A major determinant of antibody-mediated neutralization is the first 27 amino acids (aa 384-410), the hypervariable region 1 (HVR1), located at the N-terminus of HCV E2 (41). This E2 segment is highly immunogenic, and antibodies against HVR1 can be detected in the majority of HCV infected individuals (51). However, antibodies to HVR1 over time select for viral variants that escape the existing antibody response (47). The limited nature of the B cell response to this region is shown in studies of HCV evolution from acute to chronic disease (10, 46). Sequential autologous serum antibodies inefficiently neutralize emerging variants, in contrast to their capacity to neutralize earlier quasispecies. Viral escape is associated with mutations within HVR1. Other negative modulators of antibody-mediated neutralization include cell-to-cell transmission, virion-associated lipoproteins, virus envelope protein-associated glycans, and the HVR1 itself; the latter can mask epitopes or limit access of virus neutralizing antibodies to their epitopes (14, 43, 44). Indeed, virions lacking HVR1 are less susceptible to neutralization by anti-SR-B1 antibodies, but are more sensitive to antibody- and soluble CD81-mediated neutralization (1, 37). It has been suggested that HVR1 partly shields CD81 binding sites and conserved epitopes mediating virus neutralization (1).

The concept of interfering antibodies is controversial but remains a possible mechanism that contributes to the development of persistent HCV infection in infected subjects (17, 42, 49, 50). In this report, we performed more extensive epitope mapping of a panel of HMAbs to a highly conserved region on the E2 glycoprotein encompassing aa 412-423, designated as HC33-related antibodies (17). Mapping by binding against a library of alanine substitution E2 mutants from aa 384 to aa 446 revealed two subsets of HC33 HMAbs. Although both subsets have contact residues within aa 412-423, one subset included a contact residue within HVR1. This raised the possibility of anti-HVR1 antibodies interfere with the neutralizing activities of antibodies to aa 412-423. Two murine MAbs were utilized to explore the relationship between anti-HVR1 and antibodies against aa 412-423. Surprisingly, the anti-HVR1 antibody inhibited the binding and neutralization of both sets of HC33 HMAbs. This interference of binding and neutralization also was observed against other broadly neutralizing HCV HMAbs that have contact residues outside of aa 412-423. Thus, immunization strategies that avoid the induction of HVR1 antibodies should increase the inhibitory activity of broadly neutralizing anti-HCV antibodies.

MATERIALS AND METHODS

Cells, viruses and antibodies. HEK-293T cells were obtained from the ATCC. Huh7.5 cells (generously provided by Dr. C. Rice, Rockefeller University) were grown in Dulbecco's modified minimal essential medium (Invitrogen, Carlsbad, CA), supplemented with 10% fetal calf serum (Sigma-Aldrich Co., St. Louis, MO) and 2 mM glutamine. The genotype 1a HJ3-5 recombinant HCVcc was generously provided by Dr. Stanley Lemon (University of North Carolina at Chapel Hill) (48). HMAbs CBH-7, HC-1, HC-11, HC84.20, HC84.20, HC-84.26, HC33.1, HC33.4, HC33.8 and HC33.29 against HCV E2 glycoprotein were produced as described (13, 17, 22-24). Mouse MAbs H77.16 and H77.39 and their Fab fragments against HCV E2 glycoprotein were produced as described (38).

Binding to E2 glycoprotein. A standard ELISA was used (24) to compare HMAb binding to wt and ΔHVR1 HCV E2 glycoproteins. In some experiments, incubations were performed at different temperature or in different sequence when paired with H77.16. Briefly, ELISA plates were coated with *Galanthus nivalis* lectin (GNA) and blocked with 2.5% non-fat dry milk and 2.5% normal goat serum in PBS supplemented with 0.1% Tween 20. Lysates of cells expressing HCV E2 glycoproteins were captured by GNA onto the microtiter plate, followed by incubation with HMAbs and then washing. Bound HMAb was detected by incubation with alkaline phosphatase-conjugated goat-anti-human IgG (Promega; Madison, WI), followed by incubation with *p*-nitrophenyl phosphate (Sigma) for color development. Absorbance was measured at

405/570 nm. The assay was carried out in triplicate in three independent assays for each HMAb.

Inhibition assay. An ELISA measured the inhibition by mouse MAbs of HMAb binding to GNA-captured E2 glycoproteins (20). Briefly, microtiter plates were coated with GNA and blocked with 2.5% BSA and 2.5% normal goat serum in 0.1% Tween-PBS. Pre-titrated mouse MAb was added to each well at a saturating concentration. After 1 h, HMAb was added at a concentration corresponding to 65%-75% of the maximal OD level, incubated for 30 min at either room temperature or at 40^0C and then washed. Bound HMAb was detected as described above. This assay was carried out in triplicate a minimum of two times for each HMAb.

Epitope mapping. Epitope mapping was performed using alanine substitution mutants of a defined E2 region (aa 404-425) by ELISA. Alanine substitution mutants were constructed in plasmids carrying the 1a H77C E1E2 coding sequence (GenBank accession nos. AF009606), as previously described (21). All mutations were confirmed by DNA sequence analysis (Elim Biopharmaceuticals, Inc. Hayward, CA) for the desired mutation and for exclusion of unexpected residue changes in the full-length E1-E2 encoding sequence. The resulting plasmids were transfected into HEK293T cells for transient protein expression using the calcium-phosphate method, as suggested by the manufacturer (Clontech, Mountain View, CA).

Antibody cooperativity for virus neutralization. Synergistic, additive or antagonistic cooperativity by two antibodies for virus neutralization was evaluated by the median-effect analysis method, as described (5, 6) using the CompuSyn software (ComboSyn Inc, Paramus, New Jersey). The approach takes into account the potency, the shape and the slope of the dose-dependent neutralization curve of each antibody alone and in combination, at a constant ratio, to calculate a CI. A CI value of 1 indicates additive effect, <1 indicates synergism and >1 indicates antagonism. For each antibody, dose-dependent neutralization was measured initially to determine the concentration that resulted in 50% reduction (IC_{50} value). The constant ratio of the combined antibodies was set by the IC_{50} values of the two antibodies. Neutralization of a serial two-fold dilution of each antibody and in combination was then measured in a range of concentrations above and below the IC_{50} values. The measured neutralization values were entered in the program as fractional effect (FA) in the range 0.01<FA<0.99 for each of the two antibodies and in combination. The software determines the linear correlation coefficient, *r*, of each curve to indicate the fit or conformity of the data with respect to the median-effect method and calculates the CI values in relation to FA values. The 1a HCVcc and each HMAb or combination of HMAbs were incubated for 1 h at 37°C and then plated onto Huh7.5 cell monolayers (3.2 x 10^4 cells/well) that were grown in 8-well chamber slides (Nalge Nunc,

Rochester, NY) for virus neutralization assay as described previously (17). These assays were carried out in four replicates for each HMAb and combination of HMAbs.

Production and purification of recombinant Fab molecules HC33.4 and HC33.8. Synthetic genes that were codon optimized for *Drosophila melanogaster* encoding for heavy and light chains of the Fab regions of each antibody were cloned into a Drosophila S2 Fab expression vector containing a double Strep tag for efficient affinity purification. Drosophila S2 cells were transfected with these plasmids as reported previously (15). For large-scale production, cells were induced with 5 µM $CdCl_2$ at a density of approximately 10^7 cells/ml for 7 days, pelleted and Fabs were purified by affinity chromatography from the supernatant using a Strep Tactin Superflow column followed by size exclusion chromatography using a Superdex 200 column. Purified monomeric Fab was concentrated to approximately 25 mg/ml.

Complex formation, crystallization, data collection, structure determination and refinement. A synthetic peptide comprising residues 406-425 (PGAKQNIQLINTNGSWHINST) of the H77 strain was synthetized by GenScript (> 98% purity) and dissolved in water at 10 mg/ml. Fab-peptide complexes were formed overnight at 277^{o}K containing 12 mg/ml Fab + 2 mg/ml peptide. HC33.4-peptide complex crystals were grown at 293^{o}K using the hanging-drop vapor-diffusion method in drops containing 1 µl complex solution (14 mg/ml in 10 mM Tris pH 8.0, 150 mM NaCl) mixed with 1 µl reservoir solution containing 100 mM sodium citrate pH 5.2, 300 mM ammonium sulfate, 100 mM potassium phosphate and 1 M lithium chloride. Diffraction quality crystals of the HC33.8/peptide complex were grown at 293^{o}K as described above using a seed stock derived from HC33.4/peptide complex crystals and reservoir solution containing 32% PEG 4000, 100 mM Tris-HCl pH 8.5 and 800 mM lithium chloride with 0.5 µl of seed stock solution. Rock-like crystals appeared after one week and were flash-frozen in mother liquor with 20% glycerol. Spacegroups and cell dimensions refinement statistics are summarized in Table 1. Data were collected at the Synchrotron Soleil (Proxima 1) for the HC33.4 complex crystals and at the SLS (PX 1) for the HC33.8 complex crystals. Data were processed, scaled and reduced using XDS (16) and programs from the CCP4 suite (7). The crystal structures of the Fab complexes were determined by the molecular replacement method using Phaser (30). The molecular replacement for Fab HC33.4 was performed using separate variable and constant regions of a hypothetical Fab fragment assembled from the LC of PDB accession code 4JZO (89% aa identity) and the HC of PDB accession code 3KDM (91% aa identity) as search model. The molecular replacement for Fab HC33.8 was performed using Fab HC33.4 as search model. Model building was performed using Coot (11) and refinement was done using AutoBuster (3). Difference maps calculated after refinement of the Fab molecules revealed an unambiguous side chain density for a tryptophan residue close to the complementarity determining regions (CDRs), which allowed us to manually build a partial atomic model for the peptide comprising aa 418-421 (HC33.4 complex) and aa 415-421 (HC33.8), respectively. The atomic coordinates

and structure factors have been deposited in the Protein Data Bank, www.pdb.org, under the accession numbers 5FGB and 5FGC.

Crystal structure analysis. Peptides were aligned using the MatchMaker algorithm implemented in Chimera (36) and an iterative alignment process pruning long atom pairs until no pair exceeds 1 Å. Root mean square deviations were calculated using Chimera. Buried solvent accessible surface areas for the interfaces as well as for individual residues within the peptides were calculated using the PISA server (27). Interactions were determined using the protein interactions calculator (PIC; (45)). Figures were prepared with PyMOL (http://www.pymol.org).

Statistical analysis. Statistical tests were two-sided, and *P* values (calculated by Graphpad software) below 5% are considered significant.

RESULTS

HVR1 has different effects on blocking antibody access to epitopes on E2. HVR1 attenuates the activity of broadly neutralizing antibodies to HCV (1, 37). Its ability to decrease the potency of virus neutralizing antibodies was established with representative HMAbs to clusters of overlapping epitopes, designated as antigenic domains B and C (1). To test whether HVR1 acts by shielding access of these and other broadly neutralizing antibodies to their respective epitopes, binding studies were performed to 1a H77C recombinant E2 protein, with and without HVR1 (ΔHVR1) (Figs. 1A and 1B). Representative antigenic domain B antibodies (HC-1 and HC-11 (19)) bound to higher levels to ΔHVR1 E2 than wt E2 but with different degrees of increase (86% and 14% , P <0.05). Antigenic domain D antibodies (HC84.20, HC84.24 and HC84.26 (24)) also bound more to ΔHVR1 E2 than to wt E2 (56-75%, P <0.05). CBH-7, an antigenic domain C antibody (13) also bound higher to ΔHVR1 E2 but with only a minimal increase (6%, P <0.05).

We next interrogated HMAbs that recognize linear epitopes located in a highly conserved region on E2, encompassing aa 412-423, designated as antigenic domain E (17, 18), and observed two different patterns. HC33.1 behaved similarly to antigenic domain B and D antibodies with greater binding to ΔHVR1 E2 than wt E2 (50%, P < 0.001) (Figs. 1A and 1B). Unexpectedly, binding by three other E antibodies, HC33.4, HC33.8 and HC33.9, to ΔHVR1 E2 was reduced compared to wt E2 protein (65-78%, P <0.05). The decrease in binding of these MAbs to ΔHVR1 E2 suggests that part of their epitopes may fall within the HVR1.

Epitope mapping of antibodies to a highly conserved region on E2. Prior mapping of HC33-related HMAb epitopes was limited to aa 411-446 by alanine-scanning mutagenesis analysis of H77C E2 (17). That analysis revealed loss-of-binding residues located at L413, G418 and W420. We expanded on these results using alanine-scanning mutagenesis of aa 384-446 on E2, which included the entire HVR1 region (aa 384 to 410) (Fig. 1C). The E2 mutants were expressed in 293T cells and binding by HC33.1, HC33.4, HC33.8 and HC33.29 to cell lysates was measured by ELISA. Expression levels of the mutants were normalized by binding with CBH-17, a non-neutralizing HMAb that recognizes a different linear epitope on HCV E2 (13). A test concentration of 50% maximum binding of each antibody was selected for epitope mapping studies. This was determined by dose-dependent binding of each HC33 HMAb to E2 that showed the test concentration in the linear portion of the binding curve (data not shown). A greater than 80% reduction in binding was observed again for all four HC33-related HMAbs with alanine substitutions at L413A, G418A and W420A (Fig. 1C), which suggests that they bind to the same or to nearly identical epitopes. Three of these antibodies, HC33.4, HC33.8 and HC33.29, also showed greater than 80% reduction in binding against a K408A mutant E2 protein. Taken together, these mapping studies revealed two subsets of HC33-related antibodies, and explain why the deletion of HVR1 led to decreased binding by HC33.4, HC33.8 and HC33.29, and not HC33.1.

Anti-HVR1 antibody blocks the binding of broadly neutralizing antibodies. Epitope mapping of HC33-related antibodies revealed two subsets. One set, HC33.1, has contact residues that are restricted to aa 412-423. This is similar to other MAbs to this region, e.g. AP33, HCV1 and H77.39 (33, 38). The other set, HC33.4, HC33.8 and HC33.29, includes a putative contact residue within HVR1 that is located at aa 408. This raises the possibility that at least some anti-HVR1 antibodies can interfere with the functions of antibodies to aa 412-423 because of their spatial proximity. To test this hypothesis, blocking studies were performed with two murine MAbs, H77.39 and H77.16 (38). H77.39 binds to an epitope centered at aa 412-423 whereas H77.16 recognizes an epitope within HVR1 (38). Epitope mapping by alanine scanning mutagenesis of H77C E2 from aa 384-446 confirmed that H77.39 recognizes residues (N415, G418 and W420) restricted to aa 412-423, whereas H77.16 binds to HVR1 residues (G406, K408 and N410) (Fig. 1C). Each of these murine MAbs was tested for blocking of binding by representative antigenic domain B-E HMAbs (Fig. 2). H77C E2 was first incubated with either H77.39 or H77.16 prior to adding the test HMAb. As expected, H77.39 inhibited the binding to E2 of both subgroups of HC33 HMAbs (67-75%, $P<0.05$, (Fig. 2A). Inhibition also was observed against representative neutralizing HMAbs to two other epitope clusters. HC-1 and HC-11 (antigenic domain B) were inhibited by H77.39 between 73-74% ($P<0.05$) and HC84.24 and HC84.26 (antigenic domain D) were inhibited between 64-69% ($P<0.05$). Against a neutralizing antibody (CBH-7) to a third domain C cluster, essentially no inhibition was observed ($P>0.05$). The inhibition of domain D HMAb binding by an antibody to aa 412-423 has been observed

previously and is unidirectional, which is consistent with proximity but not overlapping nature of their respective epitopes (17).

Unexpectedly, H77.16, a murine MAb that binds primarily to 1a H77C HVR1 (38) also blocked both subsets of HC33-related HMAbs by 75-89% (P<0.05) (Fig. 2B). Although we anticipated inhibition by H77.16 against HC33.4, HC33.8 and HC33.9 because of the effect of the K408A mutation on their binding, we did not expect a loss of HC33.1 binding (Fig. 1C). H77.16 blocked antigenic domain B antibodies HC-1 and HC-11 by 51% to 53% (P<0.05) and antigenic domain D antibodies HC84.24 and HC84.26 by 39% to 44% (P<0.05). In contrast, binding by an antigenic domain C antibody, CBH-7 was not affected by H77.16 (P>0.05). Contact residues within HVR1 have not been identified for antibodies to antigenic domains B, C and D in previous studies (13, 19, 24). Thus, the global blocking effect of H77.16 on the binding of these broadly neutralizing antibodies suggests that anti-HVR1 antibodies may interfere with the neutralizing antibodies of antigenic domain B, D and E.

Anti-HVR1 interferes with broadly neutralizing antibodies. We next examined the neutralization of 1a H77 HCVcc by representative antigenic domains B-E HMAbs in the presence or absence of "interfering" HMAbs. We assessed whether combinations of antibodies were antagonistic, additive or synergistic using the median-effect analysis method, as described in Materials and Methods (5). A constant ratio between the HVR1 antibody H77.16, and HC33.1 or HC33.4 (domain E), HC-11 (domain B), HC84.26 (domain E) or CBH-7 (domain C) was set by their respective IC_{50} concentrations against the 1a H77 (HJ3-5) HCVcc (48). The IC_{50} concentrations for HC-11 (1.2 µg/ml) and HC84.26 (0.080 µg/ml) were previously established (19, 24). Dose-dependent neutralization was performed for H77.16, HC33.1, HC33.4 and CBH-7 that determined their respective IC_{50} values of 0.5, 3.24, 0.11 and 1.8 µg/ml (data not shown). Dose-dependent neutralization was tested for each antibody and in combination in a range of two-fold dilutions in concentration from 8(IC_{50}) to 1/16(IC_{50}). A representative set of analyses to determine cooperativity in virus neutralization is shown in Figures 3A-C for H77.16 and HC33.4. Dose-dependent neutralization for H77.16, HC33.4, and H77.16 + HC33.4 in combination from a dose of 8(IC_{50}) to 1/32(IC_{50}) was determined (Fig. 3A); fractional effect (FA) values were plotted in relation to dose (Fig. 3B); and combination index (CI) values were calculated and plotted in relation to fractional effect, FA (Fig. 3C). These studies were performed initially for H77.16 in combination with HC33.1, HC33.4, HC-11, HC84.26 or CBH-7. For each set of analyses, the linear correlation coefficient r was greater than 0.95 indicating a high goodness of fit to the plots (data not shown). The CI values of the paired studies at FA values of 50%, 75% and 90% effective dose (ED_{50}, ED_{75} and ED_{90}) were tabulated (Fig 3D). Aside from CBH-7, the CI values for the remaining antibodies, HC33.1, HC33.4, HC-11 or HC84.26, in combination with H77.16 at FA of ED_{50} (range: 1.44-1.84), ED_{75} (range: 1.31-2.76) and ED_{90} (range: 1.18-2.32) were all above 1, which indicates antagonism. Moderate (CI ranging between 1.2-1.45) antagonism was observed

between H77.16 and HC33.1 or HC84.26 (Fig. 4A). Stronger antagonism (ranging between 1.46-3.0) was observed between H77.16 and HC33.4 or HC-11. These findings are consistent with the ability of H77.16 to interfere with the binding of representative antigenic domain B (HC-11), D (HC84.26) and E (HC33.1 and HC33.4) HMAbs. Additive cooperativity with CI values near 1.0 (defined as 0.9-1.1) was observed between H77.16 and CBH-7, which is consistent with the minimal competition between these two antibodies (Figs.2B and 4A).

To assess whether the mass of full-length IgG binding to HVR1 decreases access of broadly neutralizing antibodies to their epitopes on E2 by steric hindrance, combination antibody studies were repeated with H77.16 Fab_2 fragments (Fig. 3D). As documented for each pair, the CI values at ED_{50}, ED_{75}, and ED_{90} were substantially lower for H77.16 Fab_2 fragments than for intact H77.16 IgG in combination with HC33.1, HC33.4, HC-11 or HC84.26. The mean CI values for combination studies with H77.16 Fab_2 ranged between 0.93-1.07 for H77.16 Fab_2 molecules, which are within the additive range (Fig. 4B). The CI values for H77.16 Fab_2 in combination with CBH-7 remained within the additive range (Fig. 3D and Fig. 4B). Because both H77.16 and HC33.4 have at least one critical residue within HVR1 by alanine substitution studies (Fig. 1C) and H77.16 Fab_2 interferes less than full-length H77.16 against HC33.4 neutralization, inhibition of binding studies were performed. The findings showed that full-length H77.16 inhibited HC33.4 binding to E2 more than H77.16 Fab_2 (P<0.05) (Fig. 4C). Thus, the mass of an intact IgG binding to an epitope in HVR1 decreases the access of broadly neutralizing antibodies to E2 to their respective epitopes.

Temperature and time of addition alters anti-HVR1 interference of binding by broadly neutralizing antibodies. Previous studies with HCV (39) and other flaviviruses (9) demonstrated that higher incubation temperatures lead to greater antibody binding to cryptic epitopes because of enhanced viral protein motion. We hypothesized that at higher temperatures binding by broadly neutralizing antibodies would be increased due to greater exposure of their epitopes and decreased steric hindrance by anti-HVR1 MAbs. Two sets of H77C E2 were first exposed to H77.16 (20 µg/ml) at room temperature (RT). One (test) set was incubated at 40^0C incubator prior to adding antigenic domain E, B and D HMAbs; the other (control) set remained at RT prior to adding the HMAbs. After 30 minutes at either RT or 40^0 C, detection of test HMAb binding was determined by ELISA. Indeed, greater binding by each antigenic domain E, B and D HMAb was observed at 40^0C than at RT, and this was associated with significantly less inhibition by H77.16 at 40^0C than at RT (P <0.05, Fig. 5A). Furthermore, we tested whether pre-incubation with either broadly neutralizing antibodies or H77.16 affected the ability of H77.16 to interfere with the binding of E, B and D HMAbs. When E2 is first incubated with each E, B or D HMAb and followed by H77.16, virtually no inhibition of binding was observed by H77.16, as expected (Fig. 5B). When E2 is first incubated by H77.16 and followed by each E, B or D HMAb, the magnitudes of inhibition by H77.16 against the domain E, B or E HMAbs were similar to the

observed inhibition, as shown in Figure 5A at RT. The control antibody, CBH-7, binding to E2 was not affected by H77.16 under either test conditions (Fig. 5B). These observations support the hypothesis of steric hindrance of binding of broadly neutralizing MAbs by anti-HVR1 MAbs.

Structure determination of Fab/peptide complexes. Because the HC33.4, HC33.8 and HC33.29 epitopes appear to overlap between HVR1 and aa 412-423, structural analysis was performed. We expressed the Fab fragments derived from HC33.4 and HC33.8 and performed co-crystallization trials of complexes containing the Fab and a peptide comprising residues 406-425 (PGAKQNIQLINTNGSWHINST) of the genotype 1a strain H77. This peptide was chosen to include all putative contacts revealed by the alanine scanning mutagenesis, i.e., residues K408, L413, G418 and W420. We obtained crystals diffracting to 1.65Å resolution (Fab HC33.4) and 1.9Å resolution (Fab HC33.8), respectively (Table 1). The structures of both complexes were determined by the molecular replacement method (see Materials and Methods for more details). Since comparison of peptides from both complexes revealed an identical amino acid backbone conformation and the peptide in the HC33.8 complex structure is more complete, we concentrated our further analysis on this complex.

Molecular determinants of Fab HC33.8 interaction with its peptide epitope. The conformation of the peptide in complex with Fab HC33.8 resembles the recently described conformation of a similar peptide in complex with Fab HC33.1 (29). The interaction between the peptide and Fab HC33.8 is dominated by the side chain of W420 that protrudes and is deeply immersed into a cavity formed by the long complementarity determining region 3 loop of the heavy chain (CDR-H3), the framework residues around CDR-H2 and the CDR-L3 loop (Figs. 6B and C). This pattern agrees with the results of the alanine scanning mutagenesis with W420 being a primary determinant of antibody binding. The second residue that is suggested by the alanine scanning mutagenesis as crucial for an antibody/E2 interaction is G418. This glycine residue makes three hydrogen bonds involving main-chain atoms, however, this cannot explain the amino acid specificity suggested by alanine scanning mutagenesis. It is more likely that the extensive flexibility of the glycine residue is required to facilitate the protrusion of the W420 side chain into the described cavity in the paratope. In contrast to the HC33.1 complex, in which electron density was observed for residues 412-423, peptide residues 412-414 of the HC33.8 complex are likely to be disordered and no evidence for further direct interactions between antibody and peptide were observed.

The peptide in the HC33.8 complex is exposed to the solvent and particularly N415 (i.e., the region directly downstream of the disordered part of the peptide) is located in a solvent channel (Fig. 6A), suggesting that crystal packing does not prevent a direct interaction between K408 and the antibody. However, the N-terminal peptide parts of the HC33.1 and HC33.8 complexes likely differ due to a short stretch at the end of β-strand *F* in the heavy chain variable

region of HC33.8 (^{101}VFTDS^{105} vs. ^{101}VSSDI^{105} in HC33.1). The distances between superposed Cα-atoms from the corresponding segments of HC33.1 and HC33.8 amount to 0.2Å and 0.6Å at residues 101 and 105, respectively, and to 4.3Å in the middle, with the HC33.8 segment bulging out. Fab HC33.1 tightly interacts with I414 in the N-terminal part of the peptide via two main chain hydrogen bonds from S^{H103}, presumably stabilizing the peptide conformation in the HC33.1 complex. The bulge observed in the HC33.8 complex prohibits this interaction, suggesting major differences in the N-terminal part of the interface. The complex structure can therefore neither confirm nor rule out a direct interaction between antibody and the N-terminal part of the peptide.

Conformation of the E2 aa415-423 peptide in complex with Fab HC33.8. The peptide in the HC33.8 complex adopts an extended conformation similar to the conformation observed in complex with the related HC33.1 Fab (29). However, this binding mode contrasts with the β-hairpin formed in complex with three independent neutralizing antibodies (26, 34) or with the extended conformation observed in complex with MAb 3/11 (31) (Fig. 7). All three backbone conformations have been observed in complex with broadly neutralizing antibodies underlining the structural flexibility at the surface of infectious virus particles. Our data suggest that different conformations of the antigenic region aa 412-423 are in equilibrium and that independent antibodies recognize this site following the principle of induced fit or conformational selection. The demonstrated conformational flexibility in this antigenic region supports the hypothesis of a temperature-dependent steric hindrance of binding of broadly neutralizing MAbs by anti-HVR1 MAbs. An intact IgG that dangles upstream of the flexible antigenic domain E, (i.e., one that binds the C-terminus of HVR1), sterically blocks binding of broadly neutralizing antibodies to adjacent epitopes.

DISCUSSION

The functional and biophysical properties of HVR1 on the E2 glycoprotein contribute to the ability of HCV to escape from immune recognition, which ultimately leads to persistent infection. The region is immunodominant and serves as a major decoy that diverts the B cell response from other more conserved regions on E2. Antibodies elicited to HVR1 are neutralizing but they are associated with rapid viral escape without compromising viral fitness. Prior studies have proposed that HVR1 structurally shields access by neutralizing antibodies to their respective epitopes (1). Our finding that broadly neutralizing HMAbs to overlapping conformational epitopes in E2 bind greater to ΔHVR1 E2 than wt E2 is consistent with this hypothesis.

The different binding patterns of a panel of HMAbs to mainly linear epitopes that are located adjacent to HVR1, encompassing aa 412-423 and designated as antigenic domain E, led to a series of studies that identified a new mechanism for HVR1 attenuation of antibody-mediated virus neutralization. We showed that when an anti-HVR1 antibody occupies its site on HVR1, access of antigenic domain E antibodies (e.g., HC33.1 and HC33.4) is compromised. Diminished access also was observed against antibodies to antigenic domains B (HC-1 and HC-11) and D (HC84.20, HC84.24 and HC84.26). The major binding regions for domains B and D have been mapped to aa 529-540 and aa 440-446, respectively (19, 24). The effect of anti-HVR1 on neutralization by antibodies recognizing antigenic domains B, D, and E antibodies was apparent in the antagonism studies by the median-effect analysis method. When the mass of the anti-HVR1 antibody was reduced as Fab_2 fragments, the observed antagonism anti-HVR1 was diminished. Furthermore, increased binding by each domains B, D and E HMAb was observed at 40^0C than at RT, which is consistent with increased exposure of their cognate epitopes due to enhanced viral or in this case, protein 'breathing' at higher temperatures (9, 39). This led to decreased interference by anti-HVR1 antibodies. The drop in antagonism with H77.16 Fab_2 against both HC33.1 and HC33.4 appears similar, although the HC33.4 epitope includes a critical residue within HVR1 by alanine substitution studies. A possible explanation is that structural studies with both antibodies are nearly identical, which means that HC33.4 does not include a true contact residue at aa 408 (29). Taken together, these findings suggest that anti-HVR1 Abs interfere with the binding of broadly neutralizing antibodies by steric hindrance. Finally, the interference by H77.16 against domain E antibodies (HC33-related HMAbs) appears greater than H77.39, although H77.39 binds to the same region as antigenic domain E antibodies (Fig. 2). The difference is probably due to the different mechanisms of interference. H77.39 directly competes for the same binding sites as the HC33-related antibodies that can be affected by the relative binding affinities of the two antibodies. In contrast, H77.16 binds to an adjacent site in which the bulk of the antibody molecule is preventing the binding of HC33-related antibodies to their respective epitopes. The extent of blockade by steric hindrance is less dependent on differences in the affinities of the competing antibodies that could be more effective with the tested antibodies. The concept of antibody-mediated interference of HCV is not new. It has been proposed that epitopes within the E2 segment encompassing aa 434-446 elicit non-neutralizing antibodies, and that these antibodies interfere with neutralizing antibodies directed at an adjacent E2 segment (aa 412-426) (49, 50). However, other studies employing similar approaches of isolating polyclonal antibodies to synthetic peptides encompassing aa 412-426 and aa 434-446 showed no interference in virus neutralization (42). The lack of interference by antibodies to aa 434-446 was assessed by combination studies of HMAbs that bind to aa 412-426 or aa 434-446 (17, 24). The median-effect analysis method was applied and determined that the effect was additive and not antagonistic (17).

We performed structural studies to further understand how the binding of anti-HVR1 MAbs interferes with broadly neutralizing antibodies. The antigenic region aa 412-423 is positioned downstream of the HVR1, which is a structurally flexible region at the N-terminus of E2. HVR1 was reported to interfere with binding of neutralizing antibodies by shielding conserved epitopes (1, 37). The different structures observed for peptides comprising aa 412-423 bound to multiple neutralizing antibodies suggests that this region also has considerable structural flexibility in the HCV particle. These observations indicate that there is a long, highly flexible region at the N-terminus of E2, which extends beyond HVR1 and includes conserved residues strongly implicated in CD81 binding. Since the majority of neutralizing epitopes within E2 is located in close proximity to this flexible region, MAbs targeting epitopes within this region likely can interfere- even in the absence of direct competition for binding residues- by steric hindrance, with binding of neutralizing antibodies to other antigenic domains within E2.

Overall, our findings indicate that in addition to a direct shielding role of HVR1, an indirect shielding role is plausible and could be exerted by antibodies binding to the extended structurally flexible region at the N-terminus of E2 (including aa 412-423). Thus, immunization strategies that avoid the generation of HVR antibodies may be needed to enable broadly neutralizing to function optimally and prevent new or control established infections.

ACKNOWLEDGEMENTS

This study was supported in part by NIH grant AI108024 to SKHF, an NIH contract (HHSN272201400058C) to MSD, and by an ANRS grant to TK.

REFERENCES

1. **Bankwitz D, Steinmann E, Bitzegeio J, Ciesek S, Friesland M, Herrmann E, Zeisel MB, Baumert TF, Keck ZY, Foung SK, Pecheur EI, Pietschmann T.** 2010. Hepatitis C virus hypervariable region 1 modulates receptor interactions, conceals the CD81 binding site, and protects conserved neutralizing epitopes. J Virol **84:**5751-5763.
2. **Bowen DG, Walker CM.** 2005. Adaptive immune responses in acute and chronic hepatitis C virus infection. Nature **436:**946-952.
3. **Bricogne G, Blanc E, Brandl M, Flensburg C, Keller P, et al.** 2010. BUSTER version 2.9. Global Phasing Ltd., Cambridge (united Kingdom).
4. **Bukh J, Miller RH, Purcell RH.** 1995. Genetic heterogeneity of hepatitis C virus: quasispecies and genotypes. Semin Liver Dis **15:**41-63.
5. **Chou TC.** 2010. Drug combination studies and their synergy quantification using the Chou-Talalay method. Cancer research **70:**440-446.
6. **Chou TC, Talalay P.** 1984. Quantitative analysis of dose-effect relationships: the combined effects of multiple drugs or enzyme inhibitors. Adv Enzyme Regul **22:**27-55.
7. **Collaborative Computational Project N.** 1994. The CCP4 suite: programs for protein crystallography. Acta Crystallogr D Biol Crystallogr **50:**760-763.
8. **de Jong YP, Dorner M, Mommersteeg MC, Xiao JW, Balazs AB, Robbins JB, Winer BY, Gerges S, Vega K, Labitt RN, Donovan BM, Giang E, Krishnan A, Chiriboga L, Charlton MR, Burton DR, Baltimore D, Law M, Rice CM, Ploss A.** 2014. Broadly neutralizing antibodies abrogate established hepatitis C virus infection. Sci Transl Med **6:**254ra129.
9. **Dowd KA, Jost CA, Durbin AP, Whitehead SS, Pierson TC.** 2011. A dynamic landscape for antibody binding modulates antibody-mediated neutralization of West Nile virus. PLoS Pathog **7:**e1002111.
10. **Dowd KA, Netski DM, Wang XH, Cox AL, Ray SC.** 2009. Selection pressure from neutralizing antibodies drives sequence evolution during acute infection with hepatitis C virus. Gastroenterology **136:**2377-2386.
11. **Emsley P, Lohkamp B, Scott WG, Cowtan K.** 2010. Features and development of Coot. Acta Crystallogr D Biol Crystallogr **66:**486-501.
12. **Farci P, Alter HJ, Wong DC, Miller RH, Govindarajan S, Engle R, Shapiro M, Purcell RH.** 1994. Prevention of hepatitis C virus infection in chimpanzees after antibody-mediated in vitro neutralization. Proc Natl Acad Sci U S A **91:**7792-7796.
13. **Hadlock KG, Lanford RE, Perkins S, Rowe J, Yang Q, Levy S, Pileri P, Abrignani S, Foung SK.** 2000. Human monoclonal antibodies that inhibit binding of hepatitis C virus E2 protein to CD81 and recognize conserved conformational epitopes. J Virol **74:**10407-10416.
14. **Helle F, Goffard A, Morel V, Duverlie G, McKeating J, Keck ZY, Foung S, Penin F, Dubuisson J, Voisset C.** 2007. The neutralizing activity of anti-hepatitis C virus antibodies is modulated by specific glycans on the E2 envelope protein. J Virol **81:**8101-8111.
15. **Johansson DX, Krey T, Andersson O.** 2012. Production of recombinant antibodies in Drosophila melanogaster S2 cells. Methods Mol Biol **907:**359-370.
16. **Kabsch W.** 1988. Automatic indexing of rotation diffraction patterns. Journal of Applied Crystallography **21:**67-71.
17. **Keck Z, Wang W, Wang Y, Lau P, Carlsen TH, Prentoe J, Xia J, Patel AH, Bukh J, Foung SK.** 2013. Cooperativity in virus neutralization by human monoclonal antibodies to two adjacent regions located at the amino terminus of hepatitis C virus E2 glycoprotein. J Virol **87:**37-51.
18. **Keck ZY, Angus AG, Wang W, Lau P, Wang Y, Gatherer D, Patel AH, Foung SK.** 2014. Non-random escape pathways from a broadly neutralizing human monoclonal antibody map to a

highly conserved region on the hepatitis C virus E2 glycoprotein encompassing amino acids 412-423. PLoS Pathog **10:**e1004297.

19. **Keck ZY, Li TK, Xia J, Gal-Tanamy M, Olson O, Li SH, Patel AH, Ball JK, Lemon SM, Foung SK.** 2008. Definition of a conserved immunodominant domain on hepatitis C virus E2 glycoprotein by neutralizing human monoclonal antibodies. J Virol **82:**6061-6066.
20. **Keck ZY, Op De Beeck A, Hadlock KG, Xia J, Li TK, Dubuisson J, Foung SK.** 2004. Hepatitis C virus E2 has three immunogenic domains containing conformational epitopes with distinct properties and biological functions. J Virol **78:**9224-9232.
21. **Keck ZY, Saha A, Xia J, Wang Y, Lau P, Krey T, Rey FA, Foung SK.** 2011. Mapping a region of hepatitis C virus E2 that is responsible for escape from neutralizing antibodies and a core CD81-binding region that does not tolerate neutralization escape mutations. J Virol **85:**10451-10463.
22. **Keck ZY, Sung VM, Perkins S, Rowe J, Paul S, Liang TJ, Lai MM, Foung SK.** 2004. Human monoclonal antibody to hepatitis C virus E1 glycoprotein that blocks virus attachment and viral infectivity. J Virol **78:**7257-7263.
23. **Keck ZY, Xia J, Cai Z, Li TK, Owsianka AM, Patel AH, Luo G, Foung SK.** 2007. Immunogenic and functional organization of hepatitis C virus (HCV) glycoprotein E2 on infectious HCV virions. J Virol **81:**1043-1047.
24. **Keck ZY, Xia J, Wang Y, Wang W, Krey T, Prentoe J, Carlsen T, Li AY, Patel AH, Lemon SM, Bukh J, Rey FA, Foung SK.** 2012. Human monoclonal antibodies to a novel cluster of conformational epitopes on HCV E2 with resistance to neutralization escape in a genotype 2a isolate. PLoS Pathog **8:**e1002653.
25. **Klevens RM, Hu DJ, Jiles R, Holmberg SD.** 2012. Evolving epidemiology of hepatitis C virus in the United States. Clin Infect Dis **55 Suppl 1:**S3-9.
26. **Kong L, Giang E, Robbins JB, Stanfield RL, Burton DR, Wilson IA, Law M.** 2012. Structural basis of hepatitis C virus neutralization by broadly neutralizing antibody HCV1. Proc Natl Acad Sci U S A **109:**9499-9504.
27. **Krissinel E, Henrick K.** 2007. Inference of macromolecular assemblies from crystalline state. J Mol Biol **372:**774-797.
28. **Law M, Maruyama T, Lewis J, Giang E, Tarr AW, Stamataki Z, Gastaminza P, Chisari FV, Jones IM, Fox RI, Ball JK, McKeating JA, Kneteman NM, Burton DR.** 2008. Broadly neutralizing antibodies protect against hepatitis C virus quasispecies challenge. Nat Med **14:**25-27.
29. **Li Y, Pierce BG, Wang Q, Keck ZY, Fuerst TR, Foung SK, Mariuzza RA.** 2015. Structural basis for penetration of the glycan shield of hepatitis C virus E2 glycoprotein by a broadly neutralizing human antibody. J Biol Chem **290:**10117-10125.
30. **McCoy AJ, Grosse-Kunstleve RW, Adams PD, Winn MD, Storoni LC, Read RJ.** 2007. Phaser crystallographic software. J Appl Crystallogr **40:**658-674.
31. **Meola A, Tarr AW, England P, Meredith LW, McClure CP, Foung SK, McKeating JA, Ball JK, Rey FA, Krey T.** 2015. Structural flexibility of a conserved antigenic region in hepatitis C virus glycoprotein E2 recognized by broadly neutralizing antibodies. J Virol **89:**2170-2181.
32. **Meuleman P, Bukh J, Verhoye L, Farhoudi A, Vanwolleghem T, Wang RY, Desombere I, Alter H, Purcell RH, Leroux-Roels G.** 2011. In vivo evaluation of the cross-genotype neutralizing activity of polyclonal antibodies against hepatitis C virus. Hepatology **53:**755-762.
33. **Owsianka A, Tarr AW, Juttla VS, Lavillette D, Bartosch B, Cosset FL, Ball JK, Patel AH.** 2005. Monoclonal antibody AP33 defines a broadly neutralizing epitope on the hepatitis C virus E2 envelope glycoprotein. J Virol **79:**11095-11104.
34. **Pantua H, Diao J, Ultsch M, Hazen M, Mathieu M, McCutcheon K, Takeda K, Date S, Cheung TK, Phung Q, Hass P, Arnott D, Hongo JA, Matthews DJ, Brown A, Patel AH, Kelley RF, Eigenbrot C,**

Kapadia SB. 2013. Glycan shifting on hepatitis C virus (HCV) E2 glycoprotein is a mechanism for escape from broadly neutralizing antibodies. J Mol Biol **425:**1899-1914.

35. **Pestka JM, Zeisel MB, Blaser E, Schurmann P, Bartosch B, Cosset FL, Patel AH, Meisel H, Baumert J, Viazov S, Rispeter K, Blum HE, Roggendorf M, Baumert TF.** 2007. Rapid induction of virus-neutralizing antibodies and viral clearance in a single-source outbreak of hepatitis C. Proc Natl Acad Sci U S A **104:**6025-6030.
36. **Pettersen EF, Goddard TD, Huang CC, Couch GS, Greenblatt DM, Meng EC, Ferrin TE.** 2004. UCSF Chimera--a visualization system for exploratory research and analysis. J Comput Chem **25:**1605-1612.
37. **Prentoe J, Jensen TB, Meuleman P, Serre SB, Scheel TK, Leroux-Roels G, Gottwein JM, Bukh J.** 2011. Hypervariable region 1 differentially impacts viability of hepatitis C virus strains of genotypes 1 to 6 and impairs virus neutralization. J Virol **85:**2224-2234.
38. **Sabo MC, Luca VC, Prentoe J, Hopcraft SE, Blight KJ, Yi M, Lemon SM, Ball JK, Bukh J, Evans MJ, Fremont DH, Diamond MS.** 2011. Neutralizing monoclonal antibodies against hepatitis C virus E2 protein bind discontinuous epitopes and inhibit infection at a postattachment step. J Virol **85:**7005-7019.
39. **Sabo MC, Luca VC, Ray S, Bukh J, Fremont DH, diamond MS.** 2012. Hepatitis C virus epitope exposure and neutralization by antibodies is affected by time and temperature. Virology **422:**174-184.
40. **Shepard CW, Finelli L, Alter MJ.** 2005. Global epidemiology of hepatitis C virus infection. Lancet Infect Dis **5:**558-567.
41. **Shimizu YK, Hijikata M, Iwamoto A, Alter HJ, Purcell RH, Yoshikura H.** 1994. Neutralizing antibodies against hepatitis C virus and the emergence of neutralization escape mutant viruses. J Virol **68:**1494-1500.
42. **Tarr AW, Urbanowicz RA, Jayaraj D, Brown RJ, McKeating JA, Irving WL, Ball JK.** 2012. Naturally occurring antibodies that recognize linear epitopes in the amino terminus of the hepatitis C virus e2 protein confer noninterfering, additive neutralization. J Virol **86:**2739-2749.
43. **Thomssen R, Bonk S, Propfe C, Heermann KH, Kochel HG, Uy A.** 1992. Association of hepatitis C virus in human sera with beta-lipoprotein. Med Microbiol Immunol (Berl) **181:**293-300.
44. **Timpe JM, Stamataki Z, Jennings A, Hu K, Farquhar MJ, Harris HJ, Schwarz A, Desombere I, Roels GL, Balfe P, McKeating JA.** 2008. Hepatitis C virus cell-cell transmission in hepatoma cells in the presence of neutralizing antibodies. Hepatology **47:**17-24.
45. **Tina KG, Bhadra R, Srinivasan N.** 2007. PIC: Protein Interactions Calculator. Nucleic Acids Res **35:**W473-476.
46. **von Hahn T, Yoon JC, Alter H, Rice CM, Rehermann B, Balfe P, McKeating JA.** 2007. Hepatitis C virus continuously escapes from neutralizing antibody and T-cell responses during chronic infection in vivo. Gastroenterology **132:**667-678.
47. **Weiner AJ, Geysen HM, Christopherson C, Hall JE, Mason TJ, Saracco G, Bonino F, Crawford K, Marion CD, Crawford KA, et al.** 1992. Evidence for immune selection of hepatitis C virus (HCV) putative envelope glycoprotein variants: potential role in chronic HCV infections. Proc Natl Acad Sci U S A **89:**3468-3472.
48. **Yi M, Villanueva RA, Thomas DL, Wakita T, Lemon SM.** 2006. Production of infectious genotype 1a hepatitis C virus (Hutchinson strain) in cultured human hepatoma cells. Proc Natl Acad Sci U S A **103:**2310-2315.
49. **Zhang P, Wu CG, Mihalik K, Virata-Theimer ML, Yu MY, Alter HJ, Feinstone SM.** 2007. Hepatitis C virus epitope-specific neutralizing antibodies in Igs prepared from human plasma. Proc Natl Acad Sci U S A **104:**8449-8454.

50. **Zhang P, Zhong L, Struble EB, Watanabe H, Kachko A, Mihalik K, Virata-Theimer ML, Alter HJ, Feinstone S, Major M.** 2009. Depletion of interfering antibodies in chronic hepatitis C patients and vaccinated chimpanzees reveals broad cross-genotype neutralizing activity. Proc Natl Acad Sci U S A **106:**7537-7541.

51. **Zibert A, Schreier E, Roggendorf M.** 1995. Antibodies in human sera specific to hypervariable region 1 of hepatitis C virus can block viral attachment. Virology **208:**653-661.

FIGURE LEGENDS

Figure 1: Binding properties of broadly neutralizing HMAbs. (A) Antibody binding to wt or ΔHVR1 recombinant E2 by ELISA. Recombinant H77C E2 cell lysate was captured by pre-coated GNA wells. Bound proteins were incubated with each test HMAb at 1 µg/ml (*x*-axis) and bound antibody was detected by anti-human antibody. The *y*-axis shows the mean optical density values for triplicate wells, the mean of three experiments ±SD. **(B)** Tabulation of difference in binding between ΔHVR1 and wt E2 with calculated *P* values. **(C)** Epitope mapping of HMAb (designated as HC33) and murine MAb (H77.39) to a highly conserved E2 region, aa 412-423, and a murine MAb to HVR1 (H77.16). E2 mutant proteins were expressed in 293T cells and cell lysates were analyzed by ELISA. HC33.1, -.8 and -.29 were tested at 0.1 µg/ml and HC33.4 at 0.05 µg/ml. The murine MAbs, H77.16 and H77.39 were tested at 0.1 µg/ml. Individual protein expression was normalized by binding of CBH-17, an HCV E2 HMAb to a linear epitope (13). The E2 region encompassing aa 384-446 was analyzed. Red indicates 0-20%, orange 21-40%, brown 41-60%, white 61-100% and green >100% binding when the residue was replaced by alanine (or glycine at aa 407), relative to binding to wt. Data are shown as mean values of two independent experiments performed in triplicate.

Figure 2: Inhibition of binding by an antibody to HVR1 against broadly neutralizing HMAbs. (A and B) Competition studies with two murine MAbs against antigenic domain B-E HMAbs. Lysates of 293T cells expressing recombinant H77C E2 were used. Unlabeled murine MAb H77.39 **(A)** or H77.16 **(B)** at 20 µg/ml was first incubated with E2 that had been immobilized on an ELISA plate (24). Test HMAb at 1 µg/ml was then added and bound HMAb was measured as described (24). The percent inhibition was based on test HMAb binding in the absence of the murine MAb. Data are shown as mean percent inhibition of two experiments performed in triplicate.

Figure 3: Effects of combined MAbs to HVR1 and representative antigenic domain B-E in neutralizing 1a H77 HCVcc. (A) Dose-dependent neutralization of H77.16, HC33.4 and combined H77.16 plus HC33.4 at a constant ratio. Antibody concentrations were two-fold dilution from 8 times their respective (IC_{50}) values to 1/32 of their respective (IC_{50}) values. The constant ratio of the combined antibodies was their IC_{50} values. On the *x*-axis, a dose of 1 is at the IC_{50} concentration. Each assay was performed in four replicates and data are shown as percent neutralization, the mean ±SD. **(B)** The fractional effect (FA) plots generated by the CompuSyn program for H77.16, HC33.4 and their combination showing dosage vs. effect. **(C)** Median effect plot of calculated combination index (CI) values (logarithmic) vs. FA values, in which log CI<0 is synergism and >0 is antagonism. **(D)** Table of CI values for combinations of each H77.16 or H77.16 Fab_2 with HC33.1, HC33.4, HC-11, HC84.26 or CBH-7 at FA values of

ED_{50}, ED_{75} and ED_{90}. Data are shown as mean percent inhibition of two experiments performed in triplicate.

Figure 4: Cooperativity in functional effects of combined antibodies to HVR1 and HMAbs antigenic domains. Average CI values at FA of 0.5, 0.75 and 0.9 ± SD for virus neutralization with intact IgG **(A)** or Fab_2 fragments **(B)** of H77.16 combined with HC33.1, HC33.4, HC-11, HC84.26 and CBH-7. Dotted lines indicate the range for antagonistic, additive or synergistic effects by their respective CI values. **(C)** Unlabeled full-length and Fab_2 MAb H77.16 at 20 µg/ml were first incubated with E2 that had been immobilized on an ELISA plate (24). Test HC33.4 HMAb at 1 µg/ml was then added and bound HMAb was measured as described (24). The percent inhibition was based on test HMAb binding in the absence of the murine MAb. Data are shown as mean percent inhibition of two experiments performed in triplicate.

Figure 5: Inhibition of broadly neutralizing antibody binding is altered by changes in temperature of incubation and by timing of exposure. Cell lysates of 293T cell expressing recombinant H77C E2 were captured by pre-coated GNA wells in duplicate sets. **(A)** Unlabeled murine MAb H77.16 at 20 µg/ml was added to both sets of ELISA plates for 30 minutes at RT (24). One set was washed with buffer at RT and the other (test) set washed with buffer at 40^0C. The test set was placed in a 40^0C incubator for 10 minutes and the control set remained at RT. Each antigenic domain E (H33.1 and H33.4), B (HC-1 and HC-11) or D (HC84.24 and HC84.26) HMAb at 1 µg/ml was then added, and after 30 min at either RT or 40^0C, bound HMAb was measured at RT as described (24). The percent inhibition in either RT or 40^0C was based on each HMAb binding in the absence of the murine MAb. **(B)** H77.16 (labeled as H77.16 1^{st}) or E, B or D HMAb (labeled as H77.16 2^{nd}) was added to E2 for 30 minutes at RT. After washing, each E, B or D HMAb was added to E2 pre-incubated with H77.16 or H77.16 was added to E2 pre-incubated with E, B or D HMAbs for an additional 30 minutes. Control antibody was CBH-7, a domain C HMAb. Detection and calculation of percent inhibition were the same as **(A)**. Data are shown as mean percent inhibition of two experiments performed in triplicate.

Figure 6: Crystal structure of Fab HC33.8-peptide complex. The crystal structure of the Fab HC33.8-peptide complex was determined to 1.9 Å resolution. **(A)** View on the crystalline environment to determine crystal packing effects. The Fab is colored in light (light chain) and dark grey (heavy chain) and shown as molecular surface. The peptide (shown as a cartoon and ramp-colored from blue to red through yellow from N- to C- terminus) interacts mainly with the heavy chain and its N-terminus is exposed in a solvent channel (arrows). **(B and C)** View on the paratope of the Fab HC33.8-peptide complex from two angles illustrating the protruding side chain of W420 in a cavity formed by CDR 3 of the heavy chain 1, 2 and 3 (CDR-H3), CDR-L3 and framework residues surrounding the CDR-H2 loop. The Fab is colored as in A, CDRs 1, 2 and 3

696 are colored in cyan, light cyan and dark green for the heavy chain and in sand, olive and yellow
697 for the light chain, respectively. The peptide is shown as a cartoon and colored by atom-type
698 (orange, red and blue for carbon, oxygen and nitrogen, respectively) and binds to the paratope
699 mostly between the long CDR-H3 loop (green) and the other heavy chain CDRs. A red ellipse
700 highlights a short stretch at the end of β-strand *F* in the heavy chain variable region that bulges
701 out in HC33.8, while it tightly interacts with the peptide in the HC33.1 complex (29). **(D)** View
702 on the peptide (shown as molecular surface and colored as in B) rotated by 120° around the
703 indicated axis with respect to panel C to illustrate how the W420 side chain protrudes from the
704 bulge in the center of the peptide.

705 **Figure 7: Conformations of the antigenic region aa 412-423.** Comparison of peptide
706 conformations observed for aa 412-423. The peptides in complex with Fabs HC33.8 (A), 3/11 (B;
707 PDB 4WHT) and HCV-1 (C; PDB 4DGV; (26) as an example for the β-hairpin conformation) are
708 shown as cartoons with the side chains shown as sticks and colored by atom-type (red and blue
709 for oxygen and nitrogen, respectively, and carbon atoms colored orange (HC33.8), grey (3/11)
710 or green (HCV1)) to illustrate the differences in the backbone conformation observed for the
711 three structures.

712

Figure 1

A

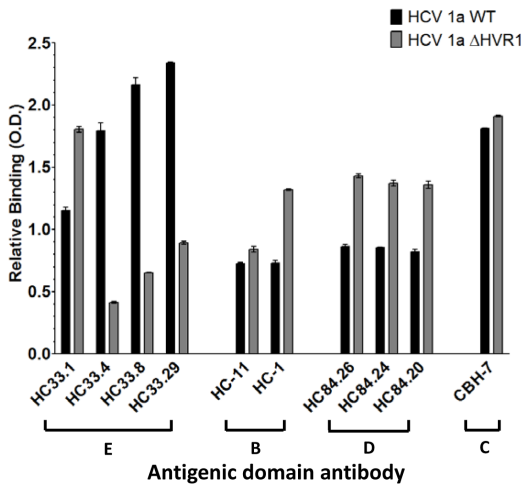

B

Antibody	Difference (%)*	P_{Value}
HC33.1	50	0.0005
HC33.4	-78	0.003
HC33.8	-68	0.002
HC33.29	-65	0.0002
HC-11	14	0.02
HC-1	86	0.001
HC84.26	56	0.0003
HC84.24	56	0.002
HC84.20	76	0.001
CBH-7	6	0.008

*Relative change in binding between ΔHVR1 and wt E2 glycoproteins.

C

	E384A	T385A	V387A	T388A	G389A	G390A	N391A	A392G	G393A	R394A	T395A	T396A	A397G	G398A	L399A	V400A	G401A	L402A	L403A	T404A	P405A	G406A	A407G	K408A	Q409A	N410A	I411A	Q412A	L413A	I414A	N415A	T416A	N417A	G418A	S419A	W42A0	H421A	I422A	N423A	S424A	T425A
H77.39	84	67	61	81	79	72	76	79	82	116	92	108	92	104	105	68	80	81	80	74	75	81	84	71	84	104	92	87	70	50	1	61	50	1	61	1	92	73	92	79	116
H77.16	89	72	62	79	69	67	68	76	67	91	79	74	71	74	74	61	61	74	75	69	38	0	61	20	79	0	79	90	98	97	83	86	82	84	82	90	91	83	81	71	93
HC33.1	103	76	84	98	86	80	94	102	92	109	93	103	101	89	102	103	103	120	107	122	93	120	107	88	98	92	119	110	11	56	137	99	119	1	142	1	100	131	107	93	135
HC33.4	78	72	79	86	81	80	87	88	82	92	86	85	86	68	95	96	58	104	105	89	76	90	96	11	88	76	95	92	7	93	106	104	103	50	127	1	116	103	93	94	111
HC33.8	104	82	121	158	91	102	107	135	128	132	127	121	96	83	115	135	101	112	113	86	78	90	100	8	84	73	102	94	17	80	134	103	125	1	156	0	136	128	111	99	123
HC33.29	132	98	141	184	102	106	115	200	170	165	159	169	123	110	134	149	137	124	119	84	86	97	96	11	79	67	90	84	25	78	100	92	101	0	118	0	107	94	87	84	90

Binding relative to wt: 0-20% | 21-40% | 41-60% | 61-100% | >100%

Figure 2

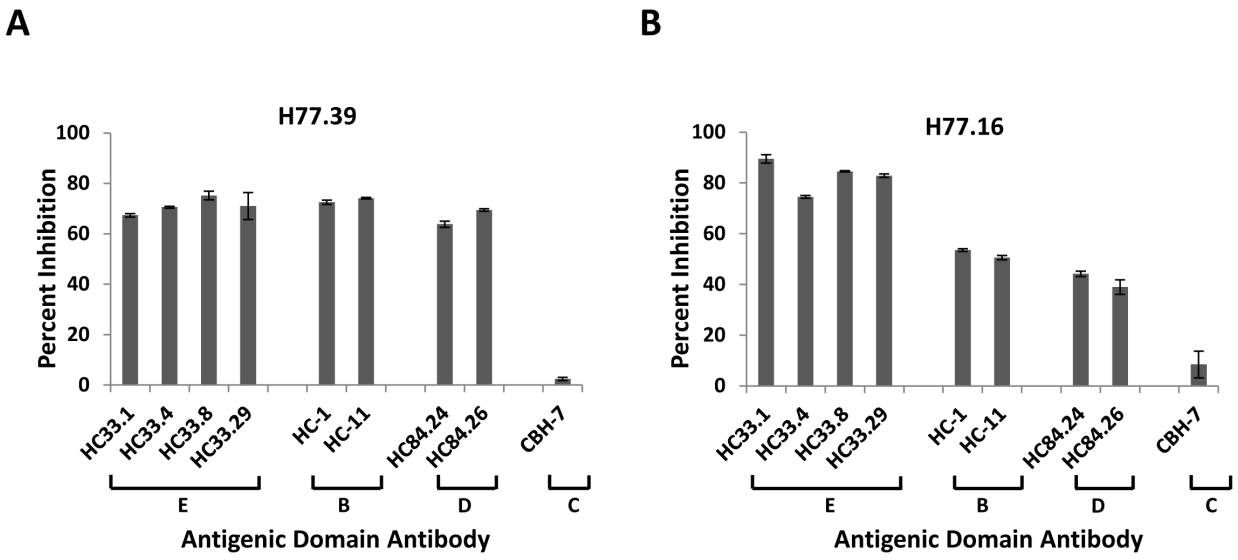

Figure 3

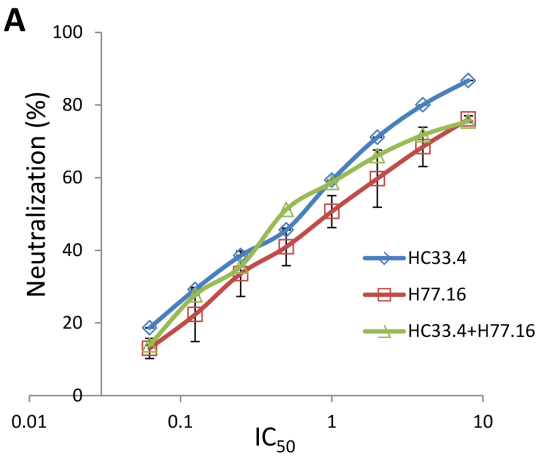

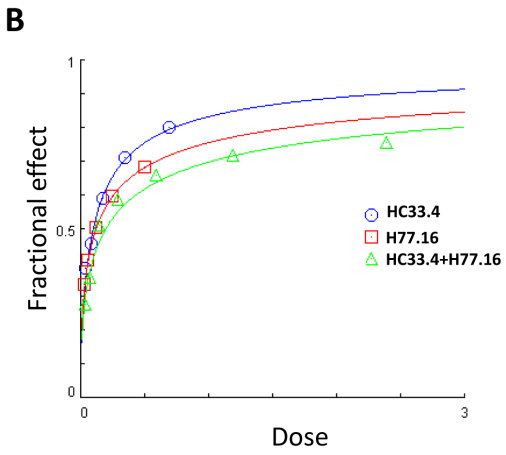

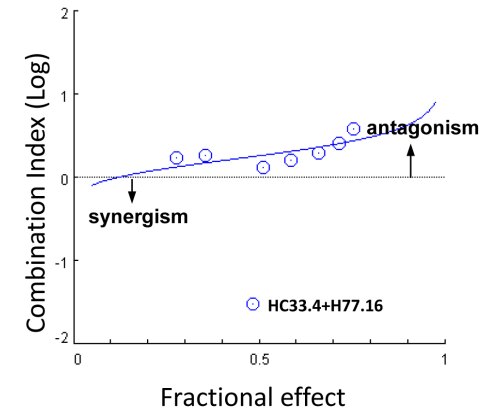

D

Combination Index for Virus Neutralization

	CI Values			
Antibody Combination	ED_{50}	ED_{75}	ED_{90}	Mean
HC33.1+H77.16	1.56	1.34	1.24	1.38
HC33.1+H77.16 Fab2	1.11	1.02	0.95	1.03
HC33.4+H77.16	1.84	2.76	2.32	2.31
HC33.4+H77.16 Fab2	0.97	1.07	1.18	1.07
HC-11+H77.16	1.44	1.48	1.59	1.50
HC-11+H77.16 Fab2	1.04	1.01	0.93	0.99
HC84.26+H77.16	1.51	1.31	1.18	1.33
HC84.26+H77.16 Fab2	0.95	0.93	0.90	0.93
CBH-7+H77.16	1.01	1.01	1.01	1.01
CBH-7+H77.16 Fab2	1.06	1.05	1.05	1.05

Figure 4

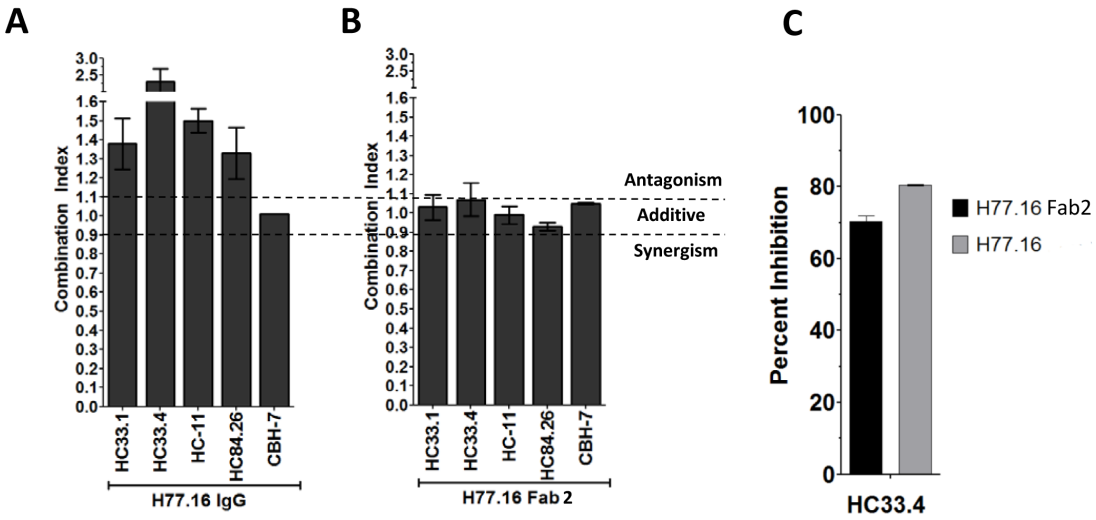

Figure 5

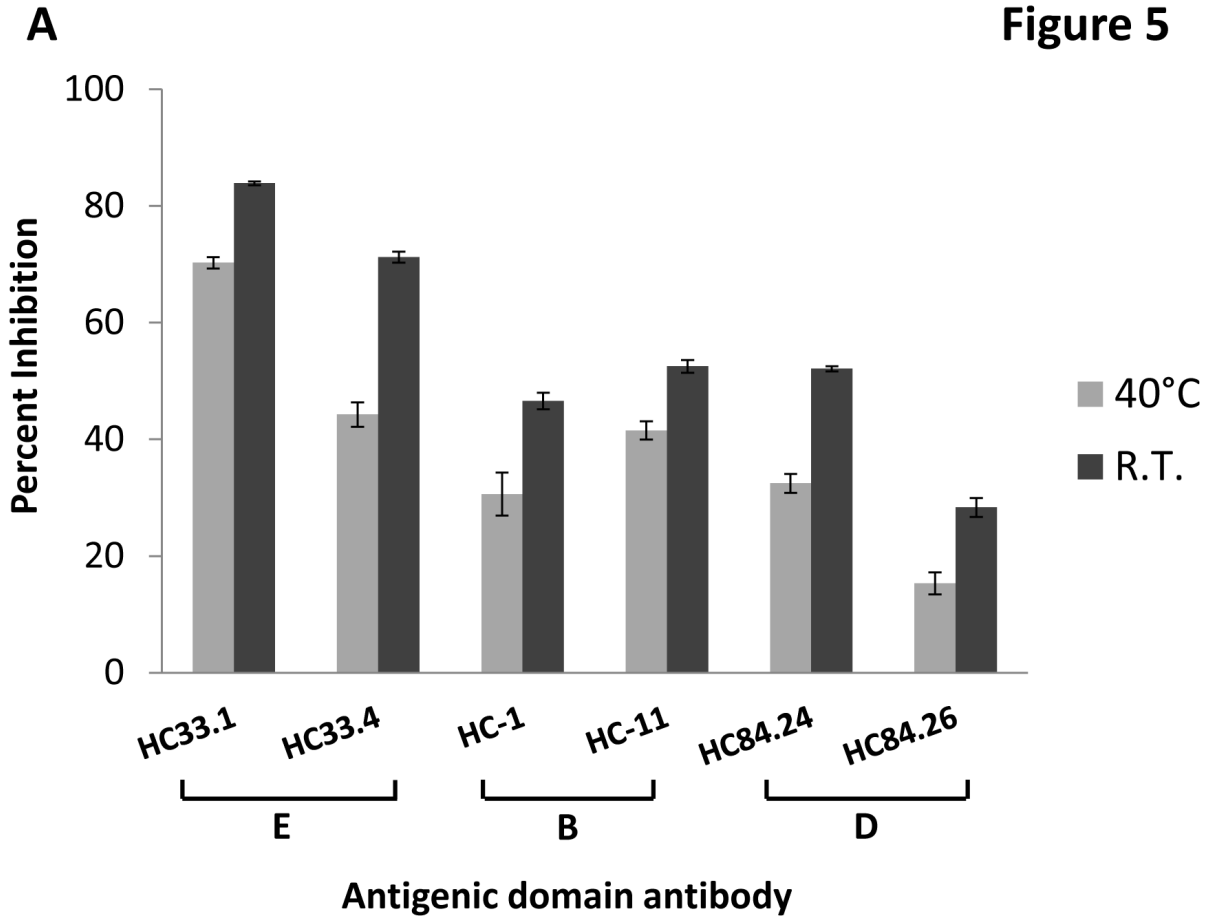

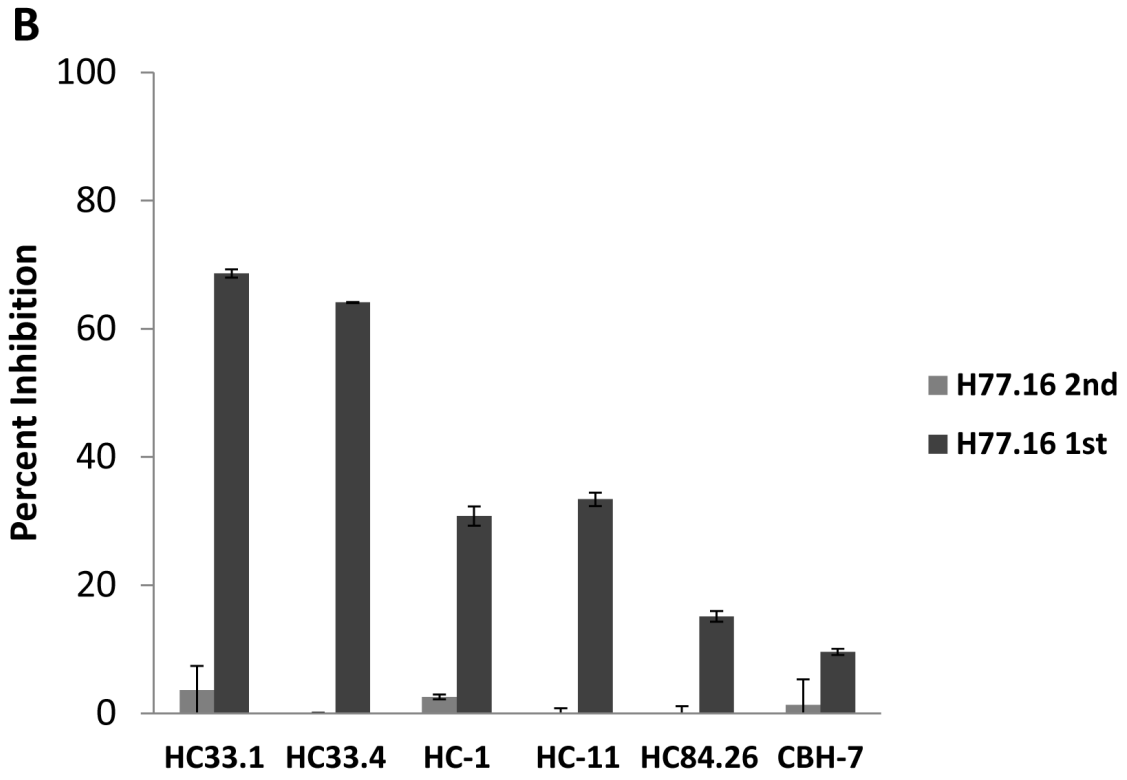

Figure 6

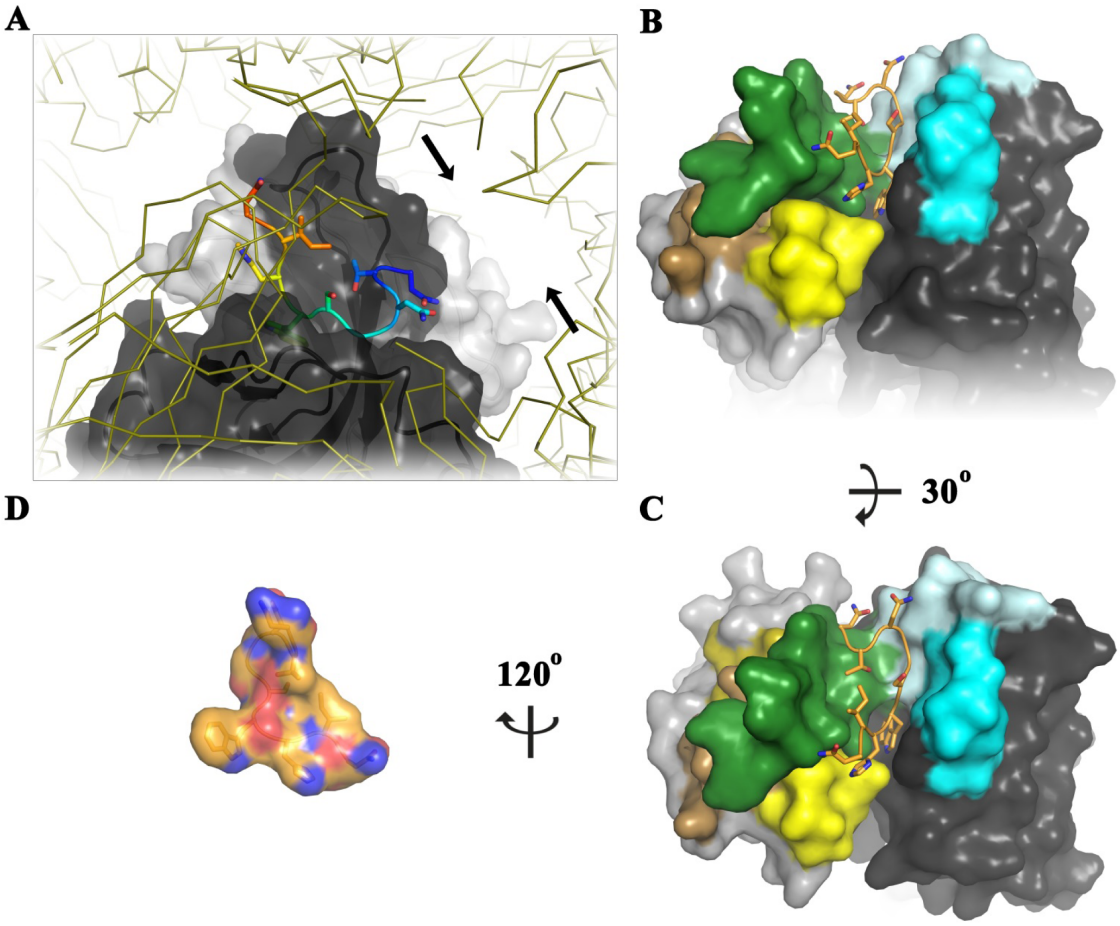

Figure 7

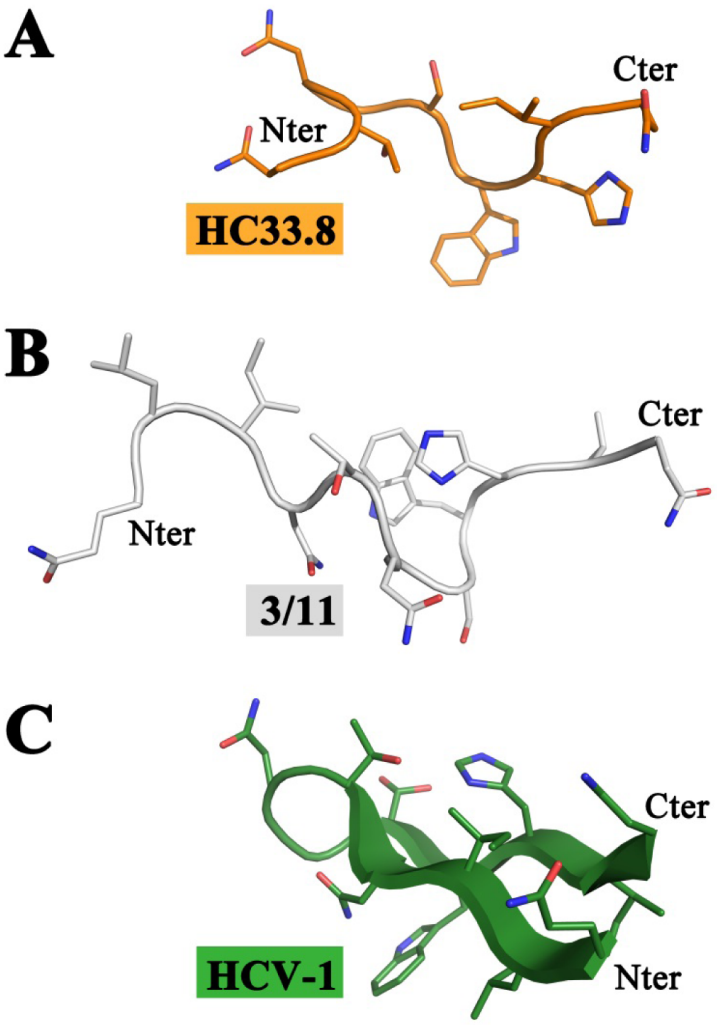

Table 1. Data collection and refinement statistics.

	Fab HC33-4 + peptide	Fab HC33-8 + peptide
Data collection		
Space group	$P2_1$	P2
Complexes per AU	2	1
Cell dimensions		
a, b, c (Å)	49.81 149.43 67.95	66.05 49.57 66.39
a, b, γ (°)	90 90.08 90	90 98.5 90
Resolution (Å)	47.25-1.65 (1.75-1.65)	49.57-1.90 (2.02-1.90)
CC(1/2)	99.8 (68.8)	99.9 (89.8)
I/ σI	12.52 (1.63)	16.17 (1.21)
Completeness (%)	99.7 (98.4)	99.6 (97.8)
Redundancy	5.3 (5.2)	6.6 (6.4)
Refinement		
Resolution (Å)	24.16-1.65	49.57-1.90
No. reflections	118727	33727
Rwork/ Rfree	0.171 / 0.189	0.194 / 0.236
No. of atoms		
Protein	6589	3414
Ligand	-	-
Water	604	116
Residues per AU	862	448
B-factors		
Protein	20.8	38.1
Ramachandran		
favored	98.00%	96.80%
allowed	2.00%	2.70%
outliers	0%	0.50%
R.m.s. deviations		
Bond length (Å)	0.01	0.01
Bond angles (°)	1.09	1.16

[1] Values in parentheses correspond to the highest resolution shell.
rmsd, root-mean-square deviation.